AERODYNAMIC INVESTIGATION OF ROTOR / PROPELLER INTERACTIONS ON A FAST ROTORCRAFT

Boisard Ronan, ronan.boisard@onera.fr, ONERA (France)

Abstract

During the past few years, different concepts of fast rotorcraft have appeared. Most of them rely on additional propellers (usually one or two of them) to ensure the propulsive force at high speed in order to be able to slow down the main rotor rotating speed. On such configuration, the propellers are in strong interaction with the main rotor wake which affects their performances and the aircraft maneuverability. The present work numerically investigates the aerodynamic of the rotor / propeller interaction on rotorcraft similar to the Racer from Airbus Helicopters. By using two different levels of modeling it is shown that at high advance ratio, a simple free wake model is perfectly able to give most of the interaction effects, while in hover, a full CFD unsteady computation may be necessary to capture all the unsteadiness of the interaction. This paper also outlines the different behavior of the propeller while it is fully inside the rotor wake or out of if, and therefore the need for a precise control of the rotorcraft in the transition between hover to fast forward flight.

NOTATION

F.W.	Free wake
c	Blade chord, m
R	Rotor radius, m
r/R	Non dimensional spanwise location
Vo	Freestream velocity, m/s
V_{tip}	Blade tip rotation velocity, m/s
μ	advance ratio, $\frac{V_o}{V_{tip}}$
Ω	Rotational velocity, rad/s
b	Number of blades
σ	Rotor solidity, $\sigma = \frac{b\,c}{\pi\,R}$
ρ	Air density, kg/m^3
S	Rotor disk surface, m²
F_X	Axial force, N
X_{bar}	Axial force coefficient, $\bar{X} = \frac{100\,F_X}{1/2\;\rho\,S\,\sigma\,(R\,\Omega)^2}$
F_z	Thrust, N
Z_{bar}	Thrust coefficient, $\bar{Z} = \frac{100\,F_Z}{1/2\;\rho\,S\,\sigma\,(R\,\Omega)^2}$
RMS	Root Mean Square: $RMS = \sqrt{\overline{X^2} - \bar{X}^2}$

1. INTRODUCTION

What makes helicopters truly unique is their capability to manage hovering flight. While this ability is extremely valuable on most of helicopters missions (operations in confined areas) this comes to a cost on the maximum reachable speed which can also become an issue for some missions (rescue operations). Nowadays conventional helicopters can usually operate up to roughly 300 km/h which is a lot less than all other fixed wing aircrafts. During the past few years, different concepts of faster rotorcraft have appeared. The first one was the X2 demonstrator by Sikorsky in 2008 (Figure 1) followed by the S-97 Raider [1],[2], which reached 370 km/h in 2015 and should lead to the SB-1 Defiant before 2020. On its side, Airbus Helicopters was even more ambitious with its X^3 demonstrator (Figure 2) which reached 472 km/h in 2013 and the Racer (Figure 3), announced for 2020, which should have a cruise speed of around 400 km/h [4].

Figure 1:Sykorsky X2

Figure 2:Airbus Helicopters X^3

Figure 3:Airbus Helicopters Racer

In any case, such high cruise speed can only be achieved by lowering the main rotor rotating speed which is then only used as a lifting device. At high speed forward flight, the propulsive force is then produced by adding one or two propellers. Depending on their position and on the rotorcraft speed, the added propellers may be more or less

Presented at 44th European Rotorcraft Forum, Delft, The Netherlands, 19-20 September, 2018

impinged by the main rotor wake. Performance of the propellers may therefore be highly dependent on the flight configurations and the aircraft maneuvering capability may also be highly altered. The objective of this paper is to investigate the aerodynamic of rotor propeller interactions on a rotorcraft similar to the X^3 or the Racer. It should provide some insight of what are the key phenomena involved, what are there effects on the propeller and main rotor characteristics and also evaluate if some simple approaches like lifting line methods are enough to capture most of the phenomena or if a full URANS CFD computation is mandatory.

2. INTERACTIONAL SETUP

Since a couple of years, ONERA has put a lot of efforts into the study of rotor/propeller wake interactions and built an experimental test rig dedicated to this topic (Figure 4).

The main rotor is based on a Dauphin helicopter test rig which was already extensively used to study rotor / fuselage interactions more than 10 years ago [5]. The propeller part is based on an off-the-shelve propeller designed for remote controlled aircraft by APC Propellers [6].

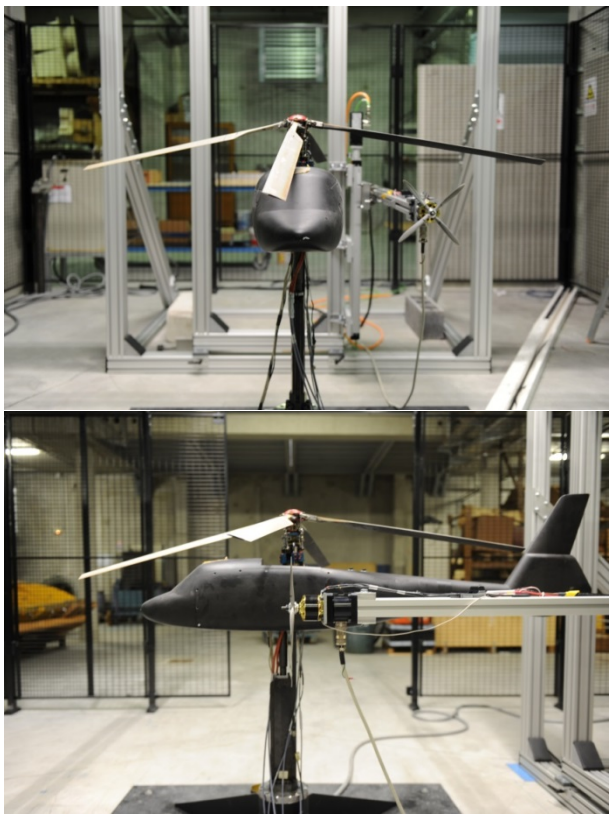

Figure 4:ONERA test rig for Rotor / Propeller wake interaction study

All the work shown here is based on this experimental setup as the computations are pre-test ones intended to be used to size the test rig and decide what are the most interesting points for measurements. The thrust and power of the propeller and main rotor will be measured using balances, and some PIV measurements are also planned in order to have a closer view of the wake interactions. This setup is scheduled to be put in the low speed L2 ONERA wind tunnel in Lille in late 2018.

2.1. The Main Rotor

The helicopter model is a 1/7.7 scale Dauphin 365N model equipped with a 4 bladed fully articulated main rotor of 1.5m diameter. In the experiment the rotor trim will be obtained by collective and cyclic pitch angles adjustment by mean of swashplate actuators. The rotor shaft is tilted 4° nose down. The blades are rectangular with a constant OA209 airfoil, a chord of 0.05m and a linear twist of -12°/R. The rotor is not Mach-scaled, and the tip speed is set to 100m/s. But this is not an issue since the main goal here is to study wake interactions at low advance ratio where compressible effects are not so important.

2.2. The Side Propeller

The propeller was chosen in order to be consistent in terms of diameter, thrust and tip speed with the main rotor compared to an actual rotorcraft of this type. It is a four bladed, fixed pitch, puller propeller of 28cm diameter made by APC Propellers. Details of the blade geometry were kindly provided by the manufacturer. The rotation speed of the propeller was set to 1/6 of the main rotor one in order to be able to have a periodic setup in the computations to ease the postprocessing and analysis of the results.

In experiment it can be added and moved around the fuselage at any position. However, for these pre-test computations, only one position of the propeller relative to the rotor was investigated. The propeller was set 0.14m ahead of the rotor center, on the rotor advancing side (0.375m from the rotor center) and 0.28m below the rotor head. This positioning is approximately what was used on the X3 helicopter from Airbus Helicopter.

2.3. Flight conditions

A target value of $Z_{bar} = 14.5$ was chosen for the main rotor. This corresponds to a medium thrust condition for which wake interactions are expected to be relatively important.

In the experiment, the rotor trim will be performed so that the axial force acting on the model will be zero ($X_{bar} = 0.$), and the lateral flapping angle will

Presented at 44th European Rotorcraft Forum, Delft, The Netherlands, 19-20 September, 2018

be zero ($\beta_{1s} = 0.$). For that purpose, static values of the rotor pitch, flap and lead-lag angles, as well as their first harmonic values are obtained from a comprehensive analysis code and used throughout all the computations. Note that the trim conditions are obtained for each advance ratio on an isolated rotor and no re-trim is performed on the installed configuration.

Concerning the advance ratio, several different operating conditions were investigated. Figure 5 shows a simple sketch of the expected rotor wake deflection in a plane passing through the propeller center for different advance ratio. In hovering condition (advance ratio 0.00) the propeller is fully immersed in the rotor wake. At advance ratio 0.05, the propeller is partially in the rotor wake and the rotor / propeller wake interactions remain extremely important. At 0.10 advance ration, the propeller itself is no longer in the rotor wake but it remains very close, and passed 0.15 advance ratio, both wakes are only slightly interacting. In the computations, only advance ratios from 0.0 to 0.25 were investigated. Moreover, 0.20 advance ratio correspond to the maximum wind speed of the wind tunnel that will be used for experiments.

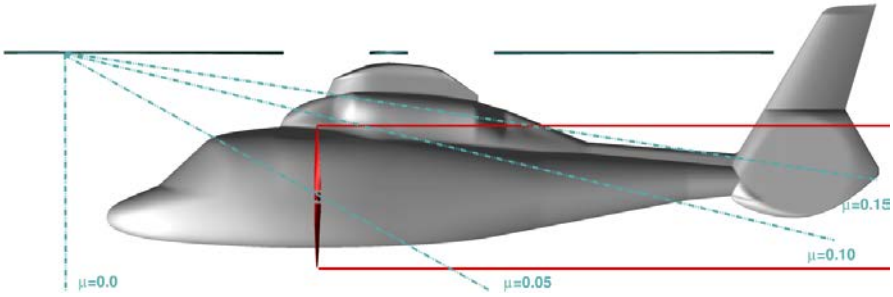

Figure 5: Sketch of isolated propeller and rotor wake path at different advance ratio

3. NUMERICAL APPROACH

In this study, two different numerical methodologies are used. The first one is a fast response method based on a lifting line approach coupled with an unsteady free wake model. The second one is much more computationally expensive and relies on URANS CFD. In the absence of any experimental results, the CFD computations will be used as reference.

3.1. Unsteady Free Wake Method

Free wake computations are based on the PUMA (Potential Unsteady Methods for Aerodynamics) code, which has been developed at ONERA since 2013. It is built on a coupling between an aerodynamic module and a kinematic module. The aerodynamic module relies on a free wake model and a lifting line approach. The free wake model is based on Mudry theory [7] which rigorously describes the unsteady evolution of a wake modelled by a potential discontinuity surface. The lifting line method relies on 2D airfoils characteristics and can handle some 3D corrections for blade sweep and 2D unsteady aerodynamics effects through dynamics stall models. Moreover, different time discretizations are available in order to balance between accuracy, scheme stability and computational time. At last, influence of any arbitrary surface onto the wake can be taken into account using a potential approach. Concerning the kinematic module, it is based on a rigid multi-body system approach using a tree-like structure with links and articulations. In order to reduce computational time, the code has been parallelized using OpenMP and the Multilevel Fast Multipole Method has been implemented for the computation of the velocities induced by each wake panel on any element. PUMA is extensively used at ONERA for any aerodynamic study of fixed wings and rotating wings configurations which requires low computational cost or a large amount of parametric investigations like pre-design studies. It has also recently been successfully applied for helicopter rotors wake in interactions with obstacles as discussed in [8] and [9].

The airfoil data needed for the free wake computations were computed using elsA CFD solver [10] for a constant Reynolds number over Mach number corresponding to the rotor scale. Concerning the numerical parameters used for the computations, they are based on ONERA previous experience on the use of PUMA for helicopter rotors and propellers and parametric study. The most meaningful parameters are:

- ✓ 12 radial stations for blade definition.
- ✓ 25 radial stations for wake emission using square root distribution along the span.
- ✓ 2° time steps for the rotor (12° for the propeller).
- ✓ No modelling of the helicopter fuselage and test rig.

Depending on the advance ration, between 5 to 15 wake revolutions were kept in order to

Presented at 44th European Rotorcraft Forum, Delft, The Netherlands, 19-20 September, 2018

compute the induced velocities and between 15 to 40 rotor revolutions were computed to ensure acceptable convergence, with an averaging of the loads over the last 5 main rotor revolutions. Note that even if a lot of rotor revolutions were computed, at low advance ratio, unsteadiness is quite important and no significant periodicity can be reached. Morover, for hover case, numerical parameters have to be tuned in order to stabilize the computation and the way the numerical parameters are tuned can highly affect the solution.

Free wake methods are relatively fast responding methods. However, due to the difference in terms of rotational speed between the propeller and the rotor, it is still time consuming. So two different approaches were used for the free wake computation:

- ✓ The first one, which is the classical one, consist of modeling all the propeller and the rotor blades, and performing a time marching computation with a small azimuthal step on the main rotor to ensure an acceptable azimuthal time step on the propeller. Mutual interaction is accounted for in the computation
- ✓ The second one consists of performing an isolated rotor computation with a standard time step. From this computation, the induced velocities around the rotor are averaged over one revolution and added to an isolated propeller computation with a standard time step. Computation only account for the effect of main rotor on the propeller.

While the second approach it almost 10 times faster than the first one, the following sections should provide some insight on when such approach can be used and which approximation is induced.

3.2. CFD Approach

All the URANS CFD computations are performed using the ONERA elsA software [10]. It is based on structured grid with overset approach.

The rotor and propeller blades grid are built using Pointwise® software. The rotor blade surface grid count 151 points in the chordwise direction per blade side and 231 points in the spanwise direction. The propeller blade surface grid count 159 points in the chordwise direction per blade side and 171 points in the spanwise direction. Extension of the grids around the blade is approximately 0.5 to 1.0 blade chord for a total number of mesh points of roughly 3.9 million per propeller blade and 5.8 million for each rotor blade. To be fully consistent with the free wake computations, the fuselage was not taken into account.

The background mesh is a Cartesian grid automatically generated using Octree approach. The full grid counts 9 grid levels with a one over two cell size increase between each level. The background grid extends up to roughly 10 rotor diameters in the farfield. The mesh is automatically refined in the vicinity of the blades up to a level of approximately 9% of the blade chord. A view of the mesh for advance ratio 0.10 is given in Figure 6. Depending on the test cases, the final meshes count from 300 million points to 440 million points.

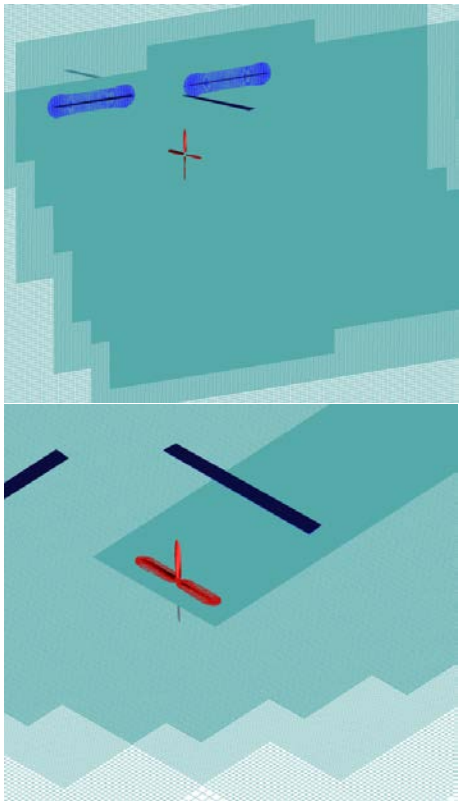

Figure 6: Iso Y (up) and Iso Z (down) view of the CFD mesh for interactional computation at μ=0.05

Computational parameters used are based on ONERA best practices on such kind of configurations. The time scheme used is a 2nd order implicit backward finite difference scheme solved by a Newton algorithm. In order to ensure good accuracy the number of Newton sub iterations was set to 25 and a physical time step corresponding to an azimuthal angle of 0.1° on the main rotor was used throughout the whole computations. Due to the low velocities involved in these computations, a 2nd order AUSM+P spatial scheme [11] was used. K-ω Wilcox model [12] was used for the turbulence with Zengh limiter and SST correction. Computations were performed in absolute velocity formulation using relative reference frame.

Presented at 44th European Rotorcraft Forum, Delft, The Netherlands, 19-20 September, 2018

While for isolated rotor and propeller computation, the convergence criteria is easy to define (no significant variations of mean thrust between two revolutions) and can be reached in relatively few rotor revolutions, it is much more difficult for the interactional setup. The hover case even seems to never reach a periodic state due to the strong interactions involved. Due to the large computational cost of such simulation, only six rotor revolutions were computed and the loads were averaged over the last one, even if it may not be fully sufficient for the hover case.

4. NUMERICAL RESULTS

Figure 7 summarizes the interactional effect on the propeller performances as a function of advance ratio computed using the free wake approach. It clearly outlines the three different interactional conditions already foreseen in Figure 5:

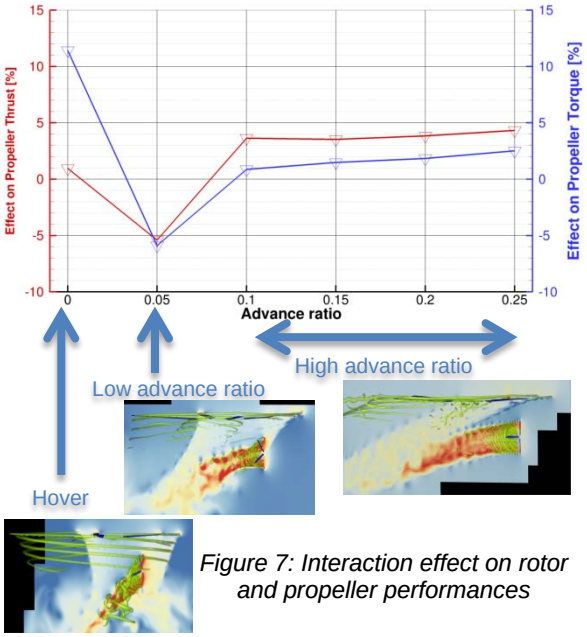

Figure 7: Interaction effect on rotor and propeller performances

- ✓ The first one is the hover case, where the propeller is fully immersed in the rotor wake, with no freestream velocity to push the rotor and propeller wake backward from the helicopter. It seems to induce large increase of torque on the propeller with no change on the mean thrust.
- ✓ The second one is the low advance ratio case, μ=0.05, for which the propeller is partially immersed in the rotor wake, but both wakes are pushed away from the rotor due to the free stream velocity. This condition is somewhat a transitional condition between hovering case and forward flight. It seems to induce a small decrease of both thrust and torque.
- ✓ The last one, for advance ratio higher than 0.10 for which the rotor wake does not directly interact with the propeller blades, and only minor wake interactions are seen. It seems to only induce very small increase of propeller thrust with almost no change on the propeller power.

Each of these three interactional conditions is investigated in more details with both free wake and CFD computations in the following sections.

In all the following sections, the thrust and power will be defined as forces and moments with respect to the vertical axis for the rotor and the horizontal axis for the propeller. In plane forces and moment, along with azimuthal blade positions will be defined with the convention given in Figure 8

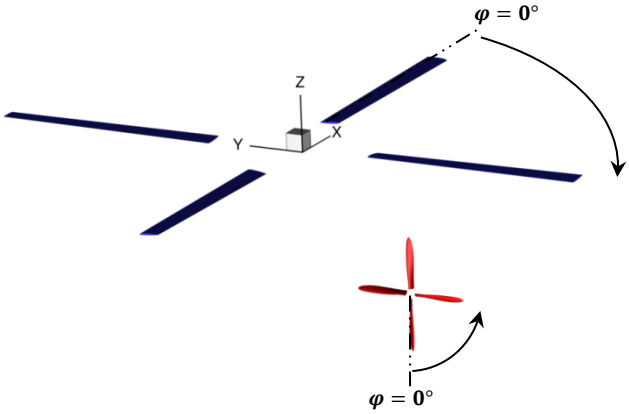

Figure 8: Rotor and propeller convention axis and orientation.

4.1. High Advance Ratio (0.10 and above)

4.1.1. Effect on propeller

Table 1 summarizes the installation effect on the propeller thrust and power for high advance ratio. Overall the rotor wake induces an increase of both the propeller thrust and the power. These gains are relatively similar for all advance ratios, with only a limited increase as the advance ratio is increasing. Moreover, the increase of thrust is always more than twice the amount of gain in power leading to an increase of propeller efficiency of more than 1 point. At last, it can be seen that both the free wake and the CFD approaches give very similar results for advance ratio 0.15.

It should be noticed that this gain in terms of performances comes with a very small increase of the loads fluctuations (Table 2). For the isolated rotor, there are absolutely no fluctuations of the thrust and power along the azimuth. On the installed case, the free wake approach does not predict any fluctuations, while in the CFD at

Presented at 44th European Rotorcraft Forum, Delft, The Netherlands, 19-20 September, 2018

advance ratio 0.15, fluctuations remain below 3% of the mean value which is quite small. Differences observed between free wake and CFD computations may come from the smaller time step used in the CFD computation and also a better modeling of the tip vortex of the main rotor.

	Propeller Thrust		Propeller Power	
	F.W.	CFD	F.W.	CFD
μ=0.10	+3.64%		+0.86%	
μ=0.15	+3.53%	+4.28%	+1.49%	+1.96%
μ=0.20	+3.84%		+1.84%	
μ=0.25	+4.32%		+2.51%	

Table 1: Installation effect on propeller thrust and power at high advance ratio

	Propeller Thrust fluctuations [%]		Propeller Power fluctuations [%]	
	F.W.	CFD	F.W.	CFD
μ=0.10	0.32%		0.20%	
μ=0.15	0.19%	2.87%	0.11%	2.82%
μ=0.20	0.24%		0.14%	
μ=0.25	0.31%		0.19%	

Table 2: Installation effect on propeller thrust and power fluctutations at high advance ratio

The reason for these increases can be relatively simply explained by looking at the rotor wake. Figure 9 details the wake from the isolated rotor at advance ratio 0.15 obtained using the free wake approach and CFD. It clearly appears that the rotor wake is passing above the propeller position and consequently it induces some reduction of the inflow velocity in the propeller plane. Moreover, the flow is almost steady with extremely small RMS in the vicinity of the propeller plane. The mean velocity is reduced by approximately 1m.s^{-1} for both computations which is almost 7% of the free stream velocity. Reducing the local inflow by keeping the same rotating speed leads to a, increase of the local angle of attack at the propeller blade leading edge, and therefore an increase of thrust. It should be kept in mind that if the propeller was already operating at its maximum thrust in the isolated case, the increase of local angle of attack could lead to flow separation and a drastic loss of thrust in the installed case.

In Figure 10 the axial, lateral and vertical velocity in the propeller plane is shown. It can be seen that while an isolated propeller is seeing a perfectly axial inflow, it is not the case anymore in the installed configuration. There is a slight downwash and sideslip of the order of 1m.s^{-1} which is equivalent to a propeller angle of attack and side slip of around 4 degrees at this free stream velocity. The RMS of the three velocity component in the propeller plane is also shown. It is quite interesting to see that the velocity is almost steady, RMS on axial, lateral and vertical velocities are below 0.1. This means that the propeller is seeing an almost steady flow, which explains the very low level of fluctuations of the propeller forces.

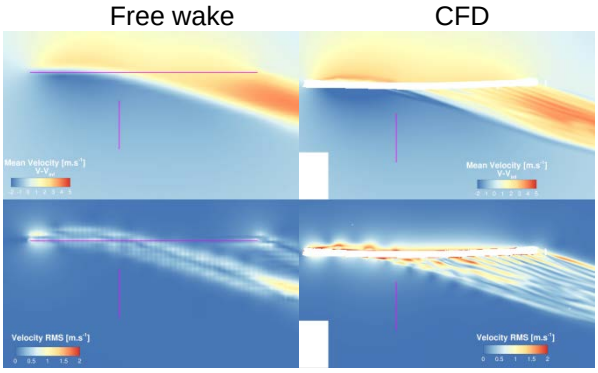

Figure 9: Mean and RMS velocity in a plane passing through the propeller center for isolated rotor at advance ratio 0.15

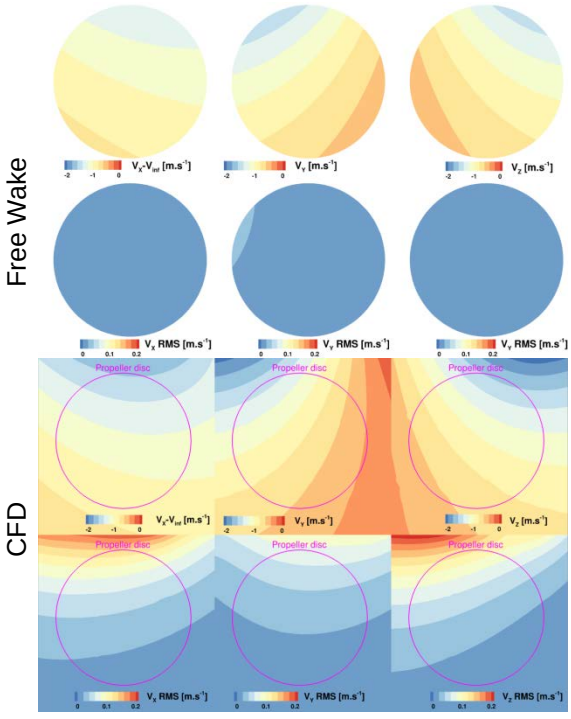

Figure 10: Mean and RMS velocity in a the propeller plane for isolated rotor at advance ratio 0.15

Due to this non axi-symmetrical flowfield there is some resulting in planes forces and moment on the propeller (Table 3). There are some

Presented at 44th European Rotorcraft Forum, Delft, The Netherlands, 19-20 September, 2018

discrepancies between free wake and CFD approaches in the prediction of these in-plane forces and moment due to the small differences in the in plane velocities. However, the order of magnitude is quite well reproduced in the free wake computation given the fact that such methods are several orders of magnitude less time consuming than CFD. Most of the in plane moment and forces a relatively small (of the order of 1 to 2 % of the one along the propeller axis). However, the pitching moment is actually non negligible since it is between 5 to 10% of the moment along the propeller axis. Depending on the position of the propeller whit respect to the rotorcraft center of gravity, this could become critical for the maneuverability.

	Fy [%Fx]	Fz	My [%Mx]	Mz
μ=0.10 F.W.	1.02	0.49	11.34	1.29
μ=0.15 F.W.	0.89	0.44	7.65	2.05
μ=0.15 CFD	0.98	0.63	5.8	2.55
μ=0.20 F.W.	0.89	0.35	6.15	1.45
μ=0.25 F.W.	1.08	0.33	5.81	1.14

Table 3: Installation effect on propeller in plane forces and moment at high advance ratio

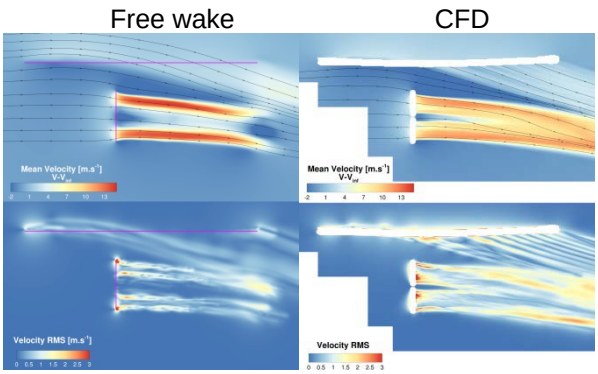

Figure 11: Details of the velocity time average and RMS in rotor and propeller wake at advance ratio 0.15

The almost steady inflow in the propeller disc anticipated by the isolated computation is confirmed by looking at the flowfield of the installed case (Figure 11). In both CFD and Free Wake computations, the main rotor wake is passing above the rotor disc and wake interactions are occurring far downstream from the propeller disc. The velocity in front of the propeller is slightly reduced and almost perfectly steady. Both computations show extremely low level of fluctuations in front of the propeller and the fluctuations seen are mainly from the propeller blade induced velocity. All these observations re-enforce the fact that in this case, it could almost be assumed that the rotor / propeller interaction is uncoupled on the propeller point of view.

Due to the "uncoupled" interaction, it is interesting to check if the numerical simulation may not be largely simplified. A simpler free wake computation was thus performed. It involves an isolated rotor computation from which a time average flowfield is extracted. Then an isolated propeller computation is performed using these surrounding flowfield. Using this approach allows to bypass the issue of the different component rotating speed and largely decreases the computational time. The results obtained are given in Table 4 and Table 5. It can be seen that the gain in terms of thrust and power are very similar with both approaches and also the in-plane forces which validates the hypothesis of an almost uncoupled phenomenon from the propeller point of view.

	Propeller Thrust	Propeller Power
μ=0.10	+3.82%	+0.89%
μ=0.15	+3.62%	+1.53%
μ=0.20	+3.89%	+1.86%
μ=0.25	+4.37%	+2.54%

Table 4: Installation effect on propeller thrust and power at high advance ratio using simplified free wake approach

	Fy [%Fx]	Fz	My [%Mx]	Mz
μ=0.10	1.05	0.63	12.79	2.8
μ=0.15	0.93	0.49	8.26	2.45
μ=0.20	0.88	0.41	6.20	1.92
μ=0.25	1.09	0.37	5.86	1.33

Table 5: Installation effect on propeller in plane forces at high advance ratio using simplified free wake approach

	Rotor Thrust		Rotor Power	
	F.W.	CFD	F.W.	CFD
μ=0.10	+0.8%		+0.9%	
μ=0.15	+0.05%	+0.54%	+1.3%	+2.86%
μ=0.20	-0.08%		+1.02%	
μ=0.25	-0.11%		+0.83%	

Table 6: Installation effect on rotor thrust and power at high advance ratio

Presented at 44th European Rotorcraft Forum, Delft, The Netherlands, 19-20 September, 2018

4.1.2. Effect on main rotor

Concerning the effect of the interaction on the main rotor, results are shown in Table 6. Using free wake approach, the propeller has no effect on the main rotor thrust except at 0.10 advance ratio for which a very small effect (below 1%) is seen. It seems to have a slightly larger effect on the main rotor power, however, it is still very small (of the order of 1%). Discrepancies between CFD and free wake approach are slightly larger than for the propeller loads. While the effect on the rotor thrust remains small using CFD, the effect on the power reach almost 3% which is not negligible. The larger effect seen in the CFD may be due to the fact that the same trim was used for CFD and free wake approach. But in CFD this trim lead to a lower rotor thrust, meaning that there is less vertical deviation of the propeller wake by the main rotor, which stays closer to the rotor disc and lead to stronger interactions.

Figure 12 shows the change in local angle of attack and thrust in free wake computation on the main rotor due to the propeller for advance ratio 0.15. It shows that the just in front of the propeller position, there is some decrease of the local angle of attack (roughly 5%) and just above the rotor wake, there is an increase of the local angle of attack which becomes even more important around the point where the propeller wake is encountering the rotor wake, at the back of the rotor disc.

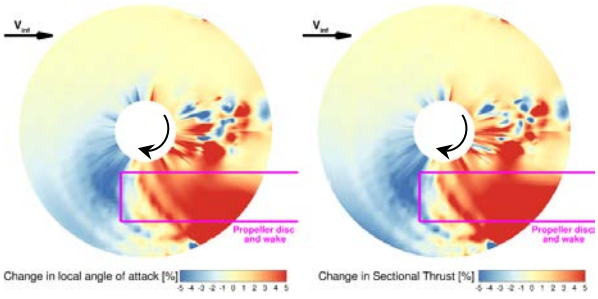

Figure 12: Change in local angle of attack and rotor thrust due the propeller for advance ratio 0.15 using free wake approach.

These changes in angle of attack are directly linked to the presence of the propeller. As seen in Figure 11 there is a suction effect of the propeller which increases the velocity just in front of it. It leads a slight increase of the velocity through the rotor disc in this area which produces the decrease of angle of attack. On the other hand, right behind the propeller, the propeller wake is producing a blockage affect which tends to lower the velocity in the rotor wake producing the local increase of angle of attack seen on the rotor blade. The blockage effect is more important when the propeller wake is encountering the rotor wake which leads to an even larger increase of angle of attack. These changes of angle of attack induce a change in the blade sectional thrust. The same effect appears on the sectional torque but it is less obvious (not shown here). There is a balancing between the increase and loss of blade sectional thrust, leading to only small amount of overall rotor thrust increase at advance ratio 0.15. When the advance ratio is larger, the miss distance between the propeller and the rotor wake will increase and the two wakes interaction will occurs more downstream. This will lead to lower blockage from the propeller wake and a smaller area of increase of rotor loads (Figure 13). But since the propeller is also operating at lower thrust, the suction effect is also smaller and so is the loss of rotor blade sectional thrust in front of it. Consequently the overall rotor thrust will be only slightly reduced.

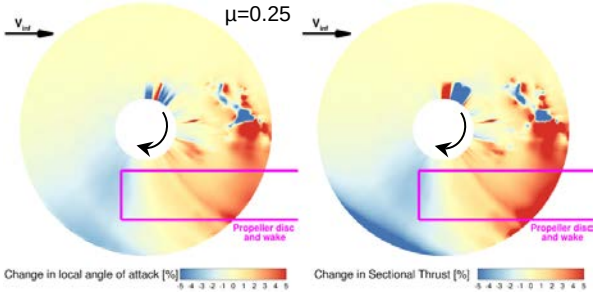

Figure 13: Change in rotor thrust due to the porpeller for advance ratio 0.25 using free wake approach.

Finally it should be noticed that due to the strong non symmetry of the thrust, on the installed case, there will be some important in plane force and moment. Even if on a real rotorcraft, there will be one propeller on each side, lowering the values of the resulting in plane forces and moments, they still will have to be balanced by a re-trim of the rotor for which high harmonic control may be necessary to handle the rapidly changing angle of attack condition on the rotor blade due to the propeller.

4.2. Low Advance Ratio (0.05)

Before going into the analysis of the results, it is important to note that for this case, the free wake approach suffers from important instabilities. The numerical parameters had to be tuned in order to avoid divergence. The number of revolutions computed had to be reduced and some cut off were introduced. The choice of these numerical parameters tuning can impact the results.

Figure 14 shows the time averaged velocity and velocity RMS for the isolated rotor at advance ratio 0.05 using the free wake and CFD approaches. In this configuration, the rotor wake

Presented at 44th European Rotorcraft Forum, Delft, The Netherlands, 19-20 September, 2018

is passing roughly in the middle of the propeller position with similar increase of mean velocity for both computations. What is very different from the high advance ratio case is that this velocity incoming in the propeller disc suffer from some fluctuations. In the free wake approach, fluctuations are only due to the tip vorticies and feature some strong fluctuations spots that are traveling through the whole propeller disc. On the CFD computations, fluctuations are lower, more homogeneous and spread over the whole rotor wake, including the tip vortices and the blade viscous wake. Moreover, in the CFD fluctuations seems to impact mainly the upper part of the propeller disc.

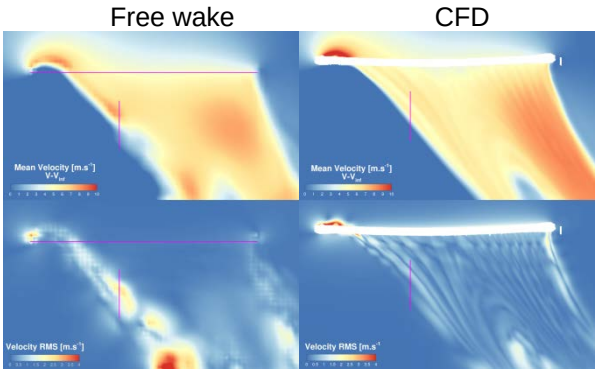

Figure 14: Mean and RMS velocity in a plane passing through the propeller center for isolated rotor at advance ratio 0.05

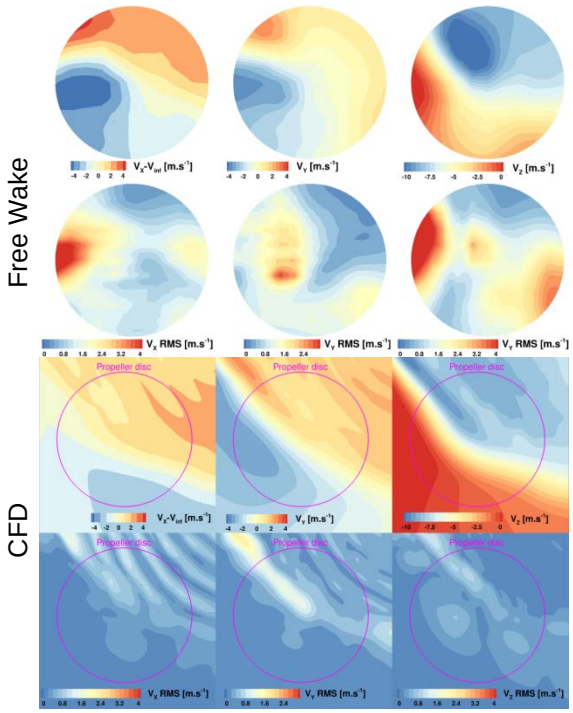

Figure 15: Mean and RMS velocity in a the propeller plane for isolated rotor at advance ratio 0.05

Figure 15 gives a detailed view of the time averaged and RMS velocity component in the propeller plane for the isolated rotor free wake and CFD computation. The overall patterns are relatively similar. However, in the free wake computation the change of axial mean velocity is much higher (up to ±4 $m.s^{-1}$) than the CFD computation (only ±2 $m.s^{-1}$) due to some spot of high velocity that are coming from the edge of the rotor wake. It should be noticed that in this case, the in plane velocities are almost twice as large as for the high advance ratio case. The lateral velocity range from -4 $m.s^{-1}$ to almost +4 $m.s^{-1}$ for both computations. But concerning the vertical velocity, the free wake approach predict a strong downwash (up to 10 $m.s^{-1}$) in the upper part of the propeller disc, probably due to main rotor tip vortex, while only a moderate downwash is seen in the CFD computation. This important in-plane velocities and the dissymmetry between the upper and lower part of the propeller disc may induce some blade stall and also some important loads unsteadiness. Concerning the fluctuating velocities, all the components are almost two times larger in the free wake approach than on the CFD computation. This is a drawback of the free wake approach in which tip vortices are very small with very high velocity and no damping through time.

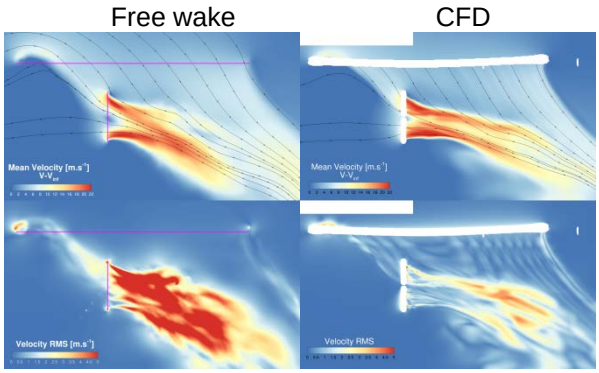

Figure 16: Mean and RMS velocity in a vertical plane passing through the propeller center for installed configurations at advance ratio 0.05

The same observations can be made on the rotor / propeller cases (Figure 16). The upper part of the propeller is directly ingesting the rotor wake which is at higher velocity than the free stream and also includes all the fluctuations from the blade wake and rotor tip vortices. The mean velocity distributions in the installed case are similar between the two computations. The propeller wake only seems to be less pushed downward in the CFD case, but it is because the trim used in the computation were the same and lead to a lower rotor thrust in the CFD than in the free wake approach. However, the fluctuations are

Presented at 44th European Rotorcraft Forum, Delft, The Netherlands, 19-20 September, 2018

much larger in front of the propeller and in the propeller wake using the free wake approach. Probably due to the large spot of fluctuations seen in the isolated case that impacts the propeller blades.

Table 7 summarizes the change in each component thrust and power with respect to the isolated case for each computation. It also gives the amount of fluctuations over the last rotor revolution for each component.

Concerning the propeller, the free wake computation predicts a loss of mean thrust of around 5%, while the CFD computation predict a small gain of thrust around 1.7%. Both computations tend to predict a loss of power, with a slightly larger amount for the CFD computation. Concerning the fluctuations, what was foreseen in Figure 14 is confirmed. The free wake approach tends to largely overestimate the fluctuations of thrust and power compared to the CFD, for which they are actually relatively low (below 5%).

		Free Wake	CFD
Propeller	Change in Thrust[1] [%]	-5.4%	+1.71%
	Fluctuations [%]	24%	4.6%
	Change in Power[1] [%]	-5.9%	-8.84%
	Fluctuations [%]	21.3%	4.9%
Rotor	Change in Thrust[2] [%]	+2.06%	+1.51%
	Fluctuations [%]	8.97%	2.23%
	Change in Power[2] [%]	+2.62%	+0.47%
	Fluctuations [%]	6.81%	1.3%

[1] Time average over six propeller revolutions
[2] Time average over one rotor revolution

Table 7: Installation effect on rotor and propeller thrust and power at low advance ratio

Looking at the time history of one blade thrust and power (Figure 17) can explain some of these discrepancies.

In the CFD computation, thrust and power are almost periodic over one propeller revolution. There is no strong impact of the rotor tip vortex passing through the propeller disc. On the opposite, for the free wake approach, the amplitude of the peak is varying a lot over one rotor revolution due to the largest fluctuations of the rotor wake velocities.

It can also be seen that the loss of thrust when the propeller blade is going down is much larger in the free wake computation than in the CFD while the power loss is relatively similar. Moreover, in the CFD the blade is regaining some thrust before reaching the vertical downward position, while for the free wake computation it does not regain any thrust before reaching the horizontal position on its way up. This is due to the vertical downward velocity seen in Figure 15. This downward velocity is larger in the free wake approach, leading to a larger loss of thrust when propeller blade is going down and to the overall loss of mean thrust of the propeller. The fact that the loss of power is similar between both approaches when blade is going down mean that in the free wake, the blade section may be close to negative angle of attack.

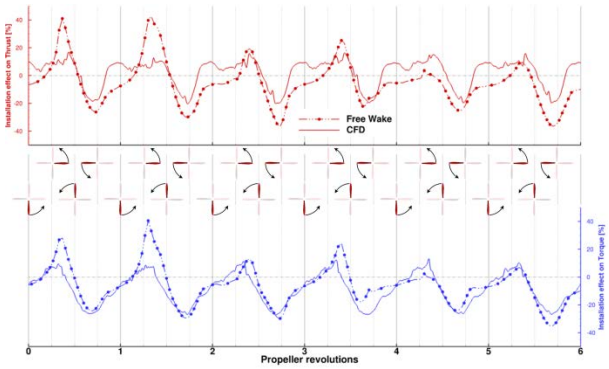

Figure 17: Time history of one propeller blade thrust and power over one rotor revolution (6 propeller revolutions)

At last, the overestimation of the peaks observed on the power explains the underestimation of the free wake approach of the average power loss.

Concerning the installation effects on the rotor (Table 7), both computations agree on an increase of both thrust and power. The predicted increase is slightly larger for the free wake approach; however it is relatively consistent with the CFD computation. Some fluctuations of the rotor thrust and power are observed, however, such fluctuations are not fully due to the propeller, since a helicopter rotor in advance flight always feature change in thrust and power around one revolution. These fluctuations are very close to the one from isolated rotor.

Figure 18 shows the loads of one rotor blade along a full revolution. Both computations give an increase of thrust and power for the rotor blade on the advancing side, with a maximum increase around the propeller position. As in the previous cases, this increase of thrust and power is due to the blockage effect of the propeller wake on the rotor. What is more surprising is that it seems that the propeller wake have also an effect on the retreating rotor blade loads. It induce some small loss of thrust and power, and in the free wake approach, it increases the blade stall (increase of power for a lower thrust). Most of the discrepancies between CFD and free wake

Presented at 44th European Rotorcraft Forum, Delft, The Netherlands, 19-20 September, 2018

computation come from the rear part of the retreating side of the rotor disc. In this area the free wake computation shows an important increase of thrust while there is absolutely no effect seen by the CFD computation. This may be linked to the convergence issues seen in the free wake approach when panels of the wake are intersecting each other which were solved by increasing numerical cut offs. The fact that the propeller has an effect on the rotor blade retreating side can be explained by looking at the velocities in an horizontal plane passing through the propeller center (Figure 19). It shows that the propeller wake is actually pushing the flow and therefore the rotor wake toward the rotor blade retreating side and it introduce some important fluctuations near the rotor blade root on the retreating side. The fact that in the free wake computation tip vortices are stronger may amplify this phenomenon leading to stronger effect on the rotor blade at the rear of the retreating side.

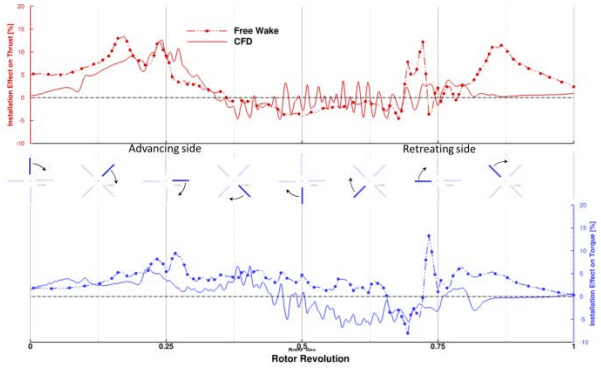

Figure 18: Time history of one rotor blade thrust and power over one rotor revolution

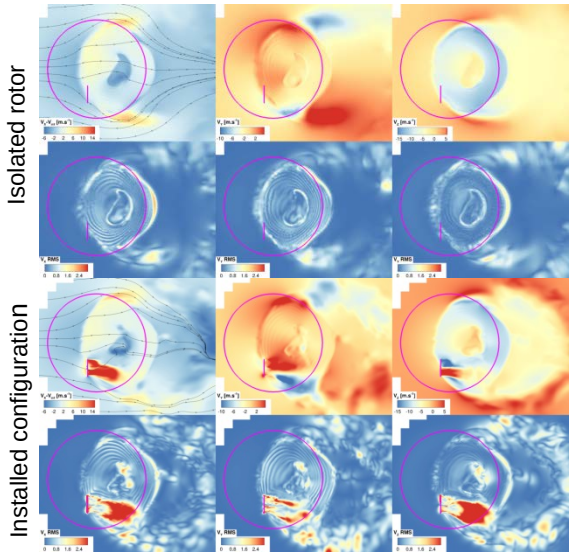

Figure 19: Mean and RMS velocity in an horizontal plane passing through the propeller center at advance ratio 0.05

4.3. Hover Case

As it was already the case for the low advance ratio, it should be reminded that for hover case, the free wake approach suffers from important instabilities and the numerical parameters had to be tuned in order to avoid divergence. The number revolutions computed had to be reduced along with the number of wake revolution kept and some cut off were introduced. The choice of these numerical parameters tuning can impact the results.

Figure 20 shows the time averaged velocity and velocity RMS for the isolated rotor in hover using the free wake and CFD approaches. In Hover the propeller disc is fully inside the rotor wake. The velocity time average in the vicinity of the propeller area is very similar in both computations, however they seem to differ in terms of RMS. The CFD computation seems to predict larger velocity fluctuations which are confirmed by looking at the velocity in the propeller disc (Figure 21). The free wake computation shows a relatively homogeneous velocity along the three components in the propeller disc, while the CFD computation predicts some gradients. Moreover, the RMS of the axial velocity component is larger in the CFD computation, but still remains relatively small. It is due to the better capability of the CFD computation to finely capture the blade wake. The downwash of the rotor is clearly visible on the vertical velocity component which is very large in the propeller disc (around 10m.s^{-1}) but with very low fluctuations. It is interesting to note that the CFD computation tends to predict a significantly lower downwash than the free wake approach on the right side of the propeller disc, which may be linked to the rotor thrust which is also lower.

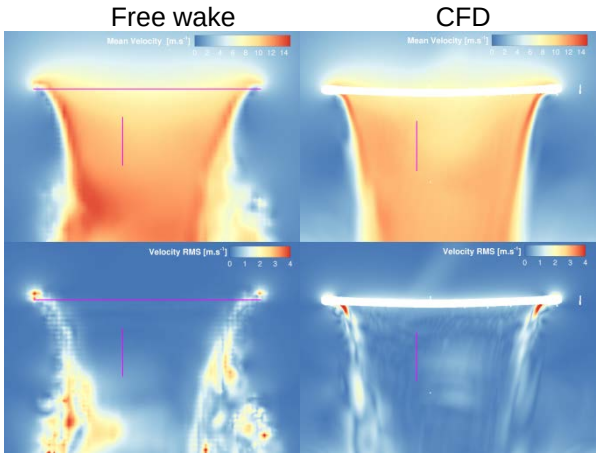

Figure 20: Mean and RMS velocity in a plane passing through the propeller center for isolated rotor in hover

Presented at 44th European Rotorcraft Forum, Delft, The Netherlands, 19-20 September, 2018

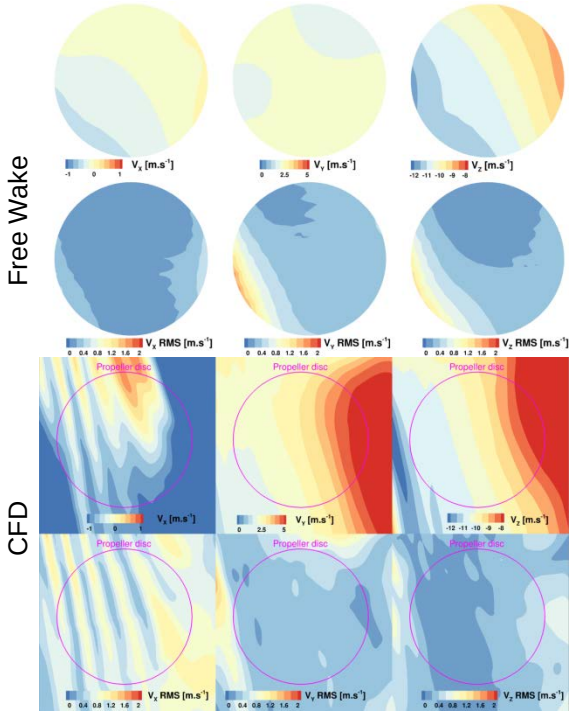

Figure 21: Mean and RMS velocity in a the propeller plane for isolated rotor at advance ratio 0.05

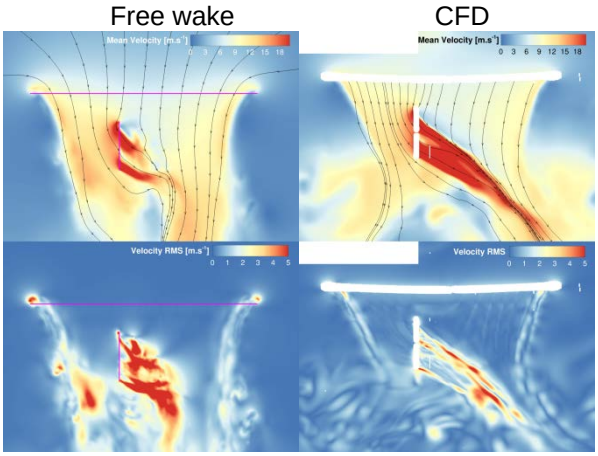

Figure 22: Mean and RMS velocity in a vertical plane passing through the propeller center for installed configurationr at advance ratio 0.05

In the previous cases, the observations made on isolated rotor enable to relatively well predict what happens in the installed case. But for hover, it is no longer the case. In the free wake computation there is relatively low effect of the propeller wake on the rotor wake but in the CFD computation, there are some strong interactions (Figure 22). In both cases, the propeller wake is pushed downward. But in the CFD computation, the rotor wake is clearly impacted by the propeller, with some larger contraction than on the rotor isolated case mainly in front of the propeller. Note that the lake of contraction observed in the free wake computation may come from the convergence issues that required to limit the number of panels in the propeller wake. Concerning the velocity RMS, as usual the free wake approach tends to overestimate the unsteadiness of the flow with very strong fluctuations just in front of the propeller disc that where not seen on the isolated case.

Table 8 summarizes the change in each component thrust and power with respect to the isolated case for each computation. It also gives the amount of fluctuations over the last rotor revolution for each component. In both computations the propeller thrust is increase, but the free wake approach tends to underestimate this increase. Concerning the power, the free wake predict a large increase (more than 12%) while the CFD computation predict a slight decrease. It seems that the free wake approach anticipate some blade stall (small increase of thrust with large increase of power) while the CFD computation tends to predict an improvement of the propeller efficiency thanks to the rotor wake. However, the increase of thrust comes with an important drawback on the load fluctuations that reach 10% of the mean value.

		Free Wake	CFD
Propeller	Change in Thrust[1] [%]	2.22%	7.72%
	Fluctuations [%]	14.47%	10.00%
	Change in Power[1] [%]	12.3%	-0.46%
	Fluctuations [%]	10.25%	8.07%
Rotor	Change in Thrust[2] [%]	-0.94 %	+2.83%
	Fluctuations [%]	4.51%	2.83%
	Change in Power[2] [%]	0.03%	0.41%
	Fluctuations [%]	1.79%	1.31%

[1] Time average over six propeller revolutions

[2] Time average over one rotor revolution

Table 8: Installation effect on rotor and propeller thrust and power at low advance ratio

Concerning the rotor performances, both computations agree on some very small changes in terms of mean thrust and power. While the free wake approach predicts a loss of almost 1% of thrust, the CFD anticipate an increase of around 3%. The fluctuations remain relatively small with some overestimation on the free wake computation.

Figure 23 shows the time history of one blade thrust and power over one rotor revolution (six blade revolutions). Loads are perfectly periodic over one propeller revolution without any effect of the rotor blade passing frequency. It appears that

Presented at 44th European Rotorcraft Forum, Delft, The Netherlands, 19-20 September, 2018

the behavior of the blade loads and power are mainly driven by the main rotor downwash. There is a gain in thrust and power on the blade up side, along with a loss of thrust and power on the blade down side. This is a characteristic of a propeller encountering an inflow with some angle of attack. The larger downwash seen in the free wake computation may lead to a loss of thrust and a raise of power on the blade up side due to the airfoil that operate a very large angle of attack, close to stall.

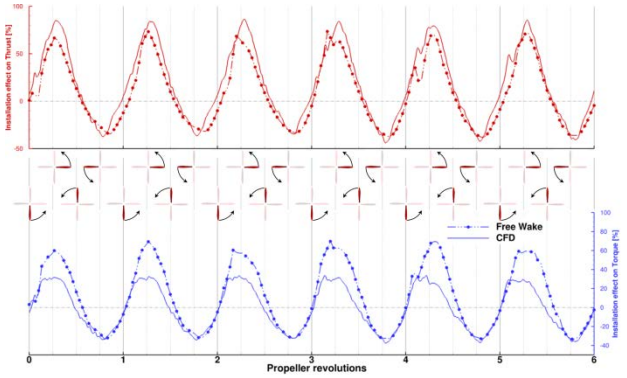

Figure 23: Time history of one propeller blade thrust and power over one rotor revolution (6 propeller revolutions)

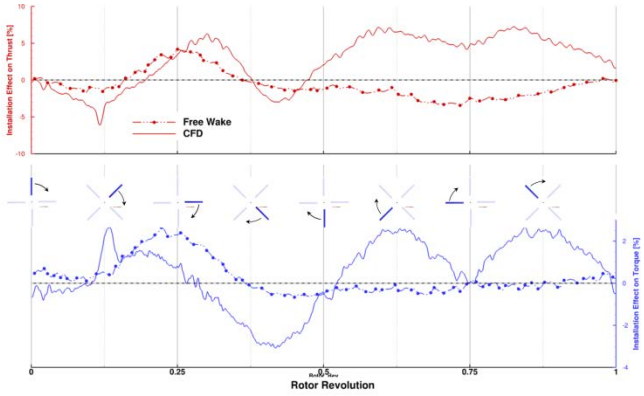

Figure 24: Time history of one rotor blade thrust and power over one rotor revolution

Figure 24 shows the time history of one rotor blade thrust and power over one rotor revolution. As for the other cases, there is a peak of thrust increase when the blade is passing above the propeller wake. The peak of power is shifted to 45 degrees azimuth at a position where there is also a loss of thrust. On the side of the propeller both computation agrees relatively well. But on the opposite side, there are some large discrepancies between free wake and CFD computations. The free wake computation does not seem to produce any effect of the propeller wake on the rotor. But on the CFD computation there is some very important effect of the wake interactions. Most of the thrust increase seems to be produced in this area at a minor cost in terms of power increase. The propeller seems to improve the rotor blade performance on this side, probably my pushing down the rotor wake and tip vortices thanks to the swirl generated in its wake. The numerical issues from the free wake computation, and mostly the number of revolutions kept in the wake may have largely modify the wake interaction leading to no effect on the rotor load on the opposite side from the propeller.

5. CONCLUSIONS

In this study, rotor / propeller wake interaction where analyzed for a given propeller position at different advance ratio. It was shown that the interactions can be classified in three different case based on the overall position of the rotor wake with respect to the propeller disc.

5.1. High advance ratio

At high advance ratio the rotor wake is passing above the propeller and does not interact directly with the propeller blades.

In this condition it was shown that the propeller encounters an increase of thrust due to the local velocity reduction produced by the rotor wake. The flow remains almost axial and only moderate in-plane forces and load fluctuations are produced. The overall rotor load is almost not affected by the propeller. Locally the rotor blade encounters some loss of sectional thrust in front of the propeller compensated by a gain of thrust while the blade is above the propeller wake.

Due to the low level of interactions between the wakes, the free wake computation is perfectly able to predict the effect on the propeller and rotor loads at a cost significantly lower than the CFD. If only the propeller loads are needed, the free wake approach can even be simplified by using a mean rotor wake flowfield.

5.2. Low advance ratio

At low advance ratio, the edge of the rotor wake is passing through the propeller disc. In this condition more discrepancies are observed between free wake computation and CFD. Fluctuations of the load are largely overestimated by the free wake approach and CFD predict a small increase of propeller thrust while the free wake lead to an important loss. Concerning the overall effect on the rotor loads, both approach leads to similar results, still with larger fluctuation for the free wake. What may not have been anticipated is the fact that there is also an effect on the rotor sectional loads on the side opposite from the propeller.

Presented at 44th European Rotorcraft Forum, Delft, The Netherlands, 19-20 September, 2018

5.3. Hover

In hover, the propeller is operating in the core of the rotor wake in a relatively steady flow dominated buy the vertical downwash from the rotor. Discrepancies between free wake and CFD are relatively large. In any cases, load fluctuations become very important due to the dissymmetry between the blade going up and the one going down. Even in this configuration effect on the rotor loads remain small but once again the rotor blade opposite to the propeller had to handle some load changes which may not have been anticipated.

Overall the free wake approach is only perfectly suitable for the high advance ratio case. At low advance ratio and in hover, the model suffers from important instabilities due to wake panel intersecting each other and the blades lifting lines. Moreover, 3D effect on the blade became extremely important and the blade often operates near blade stall leading to an increase in the discrepancies with the CFD computations.

6. ACKNOWLEDGMENTS

Part of this work was granted access to the HPC resources of CINES under the allocation 2017-A0032A10264 made by GENCI.

The author also acknowledges APC propellers for providing the geometrical description of the propeller blades.

7. REFERENCES

[1] http://raider.sikorsky.com/raider_technology_demonstrator.asp

[2] http://www.lockheedmartin.com/us/products/s-97-raider-helicopter.html

[3] D. Fournier, "Eurocopter X3, L'hélicoptère fait sa révolution", Éditions Pascal Galodé, 2014, ISBN 2355932611

[4] http://www.airbus.com/newsroom/press-releases/en/2017/06/Airbus-Helicopters-reveals-Racer-high-speed-demonstrator-configuration.html

[5] A. Le Pape, J. Gatard, J-C. Monnier, "Experimental Investigations of Rotor-Fuselage Aerodynamic Interactions." Journal of the American Helicopter Society 52.2 (2007) 99-109.

[6] https://www.apcprop.com/

[7] Mudry, M., "La théorie des nappes tourbillonnaires et ses applications à l'aérodynamique instationnaire", Thèse de Doctorat d'état, Université Paris VI, July 1982

[8] Q. Gallas, R. Boisard, J.-C. Monnier, J. Pruvost, A. Giliot, "Experimental and numerical investigation of the aerodynamic interactions between a hovering helicopter and surrounding obstacles", 43nd European rotorcraft Forum, Milan, Italy, 12-14 September, 2017

[9] R. Boisard, "Aerodynamic investigation of a helicopter rotor hovering in the vicinity of a building", 74th AHS forum, Phoenix, Arizona, USA, 14-17 May 2018.

[10] L. Cambier, S. Heib, S. Plot, "The Onera elsA CFD software: input from research and feedback from industry", Mechanics & Industry, 14, pp 159-174, 2013

[11] Liou, M.-S., Edwards, J. R., "AUSM schemes and extensions for low Mach and multiphase flows", 1999, 30th CFD Von Karman Lecture Series 1999-03

[12] Kok, J. C., "Resolving the dependence on freestream values for the k-! turbulence model", 2000, AIAA Journal 38, 1292–1295.

Presented at 44th European Rotorcraft Forum, Delft, The Netherlands, 19-20 September, 2018